Characterization of Nanosilica-Filled Epoxy Composites for Electrical and Insulation Applications

M. G. Veena,[1] N. M. Renukappa,[1] J. M. Raj,[2] C. Ranganathaiah,[2] K. N. Shivakumar[3]

[1]*Department of Electronics and Communication Engineering, Sri Jayachamarajendra College of Engineering, Mysore 570006, India*
[2]*Department of Studies in Physics, University of Mysore, Manasagangotri, Mysore 570006, India*
[3]*Center for Composite Materials Research, Department of Mechanical Engineering, North Carolina Agricultural and Technical State University, Greensboro, North Carolina 27411*

Received 12 August 2010; accepted 10 November 2010
DOI 10.1002/app.33781
Published online 29 March 2011 in Wiley Online Library (wileyonlinelibrary.com).

ABSTRACT: We report in this article the results of nanosilica (SiO_2)-filled epoxy composites with different loadings and their electrical, thermal, mechanical, and free-volume properties characterized with different techniques. The morphological features were studied by transmission electron microscopy, and differential scanning calorimetry was used to investigate the glass-transition temperature (T_g) of the nanocomposites. The properties of the nanocomposites showed that the electrical resistivity (ρ), ultimate tensile strength, and hardness of the composites increased with SiO_2 weight fraction up to 10 wt % and decreased thereafter; this suggested that the beneficial properties occurred up to this weight fraction. The temperature and seawater aging had a negative influence on ρ; that is, ρ decreased with increases in the temperature and aging. The free-volume changes (microstructural) in the composite systems correlated with seawater aging but did not correlate so well with the mechanical properties. © 2011 Wiley Periodicals, Inc. J Polym Sci Part A: Polym Chem 121: 2752–2760, 2011

Key words: crosslinking; glass transition; nanocomposites; structure–property relations; voids

INTRODUCTION

In recent years, polymer nanocomposites have attracted a great deal of attention because of their unexpected hybrid properties, which are synergistically derived from the multiple components.[1] Because of the large boundary surface created by the nanofillers, polymer composites with nanoparticles exhibit new properties that are not possible with conventional fillers. Silica-filled polymer nanocomposites have been shown to be attractive materials for microelectronics, power electronics, space devices, and other engineering applications.

The electrical characteristics of microelectronic devices, such as signal attenuation, propagation velocity, and crosstalk are influenced by the dielectric properties of the packing materials. An important role of packing material is to ensure very good electrical insulation of the silicon chip and of circuit pins. Ideally, a low-conductivity material is needed to address these issues through the prevention of current leakage, a low dielectric to minimize the capacitive coupling effects, and a low loss factor to reduce electrical losses. The industrial use of silica is widespread in applications from the microelectronics industry to nuclear technology. Because of their excellent electrical and dielectric properties, silica is extensively used in dynamic random access memory and field effect transistors.[2,3] Sun et al.[4] studied the thermal properties, moisture absorption, and dielectric properties of neat epoxy and epoxy/microsilica and epoxy/nanosilica (SiO_2) composites. They showed that the nanoparticle-filled composites had a much higher loss factor, a lower glass-transition temperature (T_g), and a higher moisture absorption than the neat and microsilica-filled epoxy composites. Zheng et al.[5] investigated the influence of SiO_2 particles on the curing reaction, T_g, dielectric behavior, and thermomechanical properties. They concluded that when SiO_2 particles were well dispersed without aggregation, they effectively increased the toughness and strength of the composites at low loadings (<3 wt %).

Zou et al.[6] prepared surface-modified epoxy–silica nanocomposites and found that the surface-modified nanoparticles reduced the water absorption in epoxy nanocomposites. However, the effect of water absorption in the nanocomposites is still far from being well understood. Because the epoxy–filler particle interface is a potential location for water

Correspondence to: C. Ranganathaiah (cr@physics.uni-mysore.ac.in).

Contract grant sponsor: All India Council for Technical Education (Delhi, India); contract grant number: 8023/BOR/RID/RPS-38/2009-10.

absorption,[7] nanocomposites with a very high specific area may be particularly vulnerable to the effects of water present at these interfaces. This possibly weakens the otherwise improved mechanical[7,8] and other properties obtained by nanofillers.

Many researchers have reported that the tensile modulus and fracture toughness of epoxy (SC 79) can be improved by the incorporation of SiO_2.[9–12] Rosso et al.[10] investigated the toughening effect of epoxy resin with SiO_2 at different temperatures. They reported a maximum of 13.6% improvement in the tensile modulus with the incorporation of 8 wt % SiO_2. Mahrholz et al.[12] also showed improved mechanical properties in SiO_2-filled epoxy composites.

However, from the literature survey on epoxy–silica-filled composites, we found that no attempt has been made to systematically understand the effect of temperature, high filler loading, and seawater aging on electrical properties. This investigation was an attempt in this direction to understand the influence of these parameters on the electrical resistivity, T_g, mechanical properties, and seawater uptake in epoxy nanocomposites. Because the microstructure controls all of these properties, with a view to understanding the microstructure and its influence on the previously mentioned properties, we made free-volume measurements using positron annihilation lifetime spectroscopy (PALS), a sophisticated tool used for the direct measurement of nanometer sized free-volume holes and their relative number densities; this technology is popularly used in the fields of polymers, polymer blends, and polymer microcomposites and nanocomposites.[13–16] We hoped that this study would shed light on the behavior of nanodielectric composites used in microelectronic devices, which can be under volatile conditions, such as seawater corrosion. Secondly, we found that positron lifetime experiments on polymer–SiO_2 nanocomposites are scanty and have been reported for only a few polymer–SiO_2 systems.

EXPERIMENTAL

Materials

The epoxy resin SC 79 (SC 79 part A, diglycidyl ether of bisphenol A) was used to fabricate nanocomposites with an epoxy equivalent weight of 162 g/mol. We used a cycloaliphatic amine (SC 79 part B) with an amine hydrogen equivalent weight of 64.8 g/mol as the hardener/curing agent. Both the resin and curing agent were supplied by Applied Poleramic, Inc. (Benicia, California)[17] The densities of the resin (SC 79 part A) and the curing agent (SC 79 part B) were 1.17 and 0.95 g/cm^3, respectively. The viscosity at 23°C was 320 cps, which increased to 950 cps after 7 h.[18] Nanopox F400 from Nanoresins AG (Charlottenburger, Geesthacht, Germany),[19] with an epoxy equivalent weight of 295 g/mol[20] nanofiller, was used in this study. It had a concentration of 40 wt % silica nanoparticles in a diglycidyl ether of bisphenol A epoxy resin. This product was supplied as colloidal silica sol in epoxy resin prepared with a sol–gel process. Samples of Nanopox (according to the data sheet of the supplier) calculated to have 5, 10, 15, and 20 wt % silica were used in our composite samples.

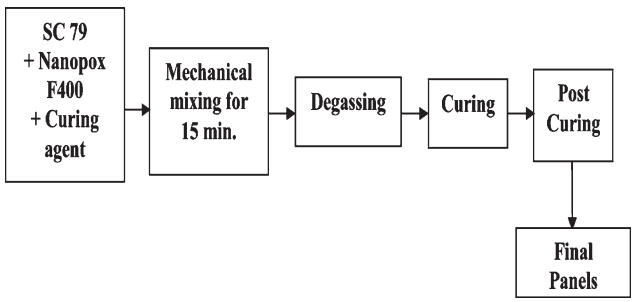

Figure 1 Flowchart for the processing of the epoxy–silica nanocomposites.

Nanocomposite fabrication

The processing flowchart of the epoxy–silica nanocomposite preparation is shown in Figure 1. The required quantity of epoxy resin and Nanopox F400 were measured and preheated separately at 60°C for 2 h. The mixture was gently stirred for 15 min with a mechanical stirrer (<1000 rpm) with the addition of SC 79B. The mixture was then degassed in a vacuum oven under a pressure of 762 mmHg to eliminate the entrapped air molecules (bubbles). Then, the composite was molded into a flat plate and cured in the oven. The curing temperature was increased with a ramp rate of 5°C/min to 60°C and vitrified for 4 h; thereafter, it was decreased to room temperature at a ramp rate of 1°C/min. The panels were then postcured at a ramp rate of 2.5°C/min to 60°C. Then, the ramp rate was changed to 1°C/3 min until a temperature of 90°C was attained. Thereafter it was changed to 1°C/min up to 120°C and remained at this temperature for 1 h. Finally, the temperature was decreased to room temperature at a ramp rate of 1°C/min. With the aforementioned process, both neat and SiO_2-modified epoxy nanocomposite panels were fabricated.

Measurements

Transmission electron microscopy (TEM)

The dispersion of SiO_2 particles in the epoxy matrix was evaluated with TEM images taken by a Jeol Ltd. (Tokyo, Japan) 100 CXII system with standard

magnification of 360 to 320,000×. There were some microvoids of various sizes in the nanometer range found in all of the nanocomposites.

Differential scanning calorimetry (DSC)

We used DSC (TA Instruments, DSC model 821, New Castle, Delaware) to study the thermal stability of the sample by measuring the T_g values of the pure epoxy and the composites. DSC, operated under a nitrogen atmosphere at a heating rate of 10°C/min in the temperature range 50–200°C, was used to determine T_g. Approximately, 6 mg of each sample was used in the experiment.

Mechanical and resistivity measurements

An Instron Corp., (Canton, Massachusetts) 4204 machine was used to conduct the tensile test at room temperature. A machine displacement rate of 1.27 mm/min was used for the test, and the specimens were loaded until failure. An average of five tests is reported here. The direct-current (dc) resistance measurements were performed under an applied voltage range of 200–1000 V in steps of 200 V with an electrification time of 180 s with an Eltel-Automatic Dielectric Constant, Tandelta, and Resistivity Test Set kit type -ADTR-2K (EL TEL, Bengaluru, India).

Seawater aging

Seawater aging was carried out by the placement of the epoxy nanocomposite specimens in a seawater bath and maintenance of a relative humidity of 95% at a constant temperature of 25°C with a laboratory humidity chamber manufactured by M/s C. M. Equipment and Instruments (India) Pvt., Ltd. (Bengaluru, India). The aging of the samples was done for 48 and 96 h. After the aging time, the samples were removed from the seawater bath and cleaned with blotting paper to remove water on the surface, and then, the electrical measurements were carried out.

PALS measurements

PALS was done for the pure epoxy and epoxy–silica nanocomposites. The spectrometer consisted of a fast–fast coincidence system consisting of BaF_2 scintillators (Scionix, Bunnik, Holland) coupled to photomultiplier tubes type XP 2020/Q with quartz windows as detectors. The BaF_2 scintillators were conically shaped to achieve a better time resolution. Two identical pieces of the sample were placed on either side of a 17-μCi ^{22}Na positron source, which was deposited onto a pure Kapton foil 12.7 μm thick. This sample-source sandwich was placed between the two detectors of the spectrometer to acquire the lifetime spectrum. The operation details, data acquisition, free-volume parameter calculation, and so on can be found in Refs. 21 and 22.

RESULTS AND DISCUSSION

The assessment of the nanoparticle dispersion and morphology can be understood from the TEM pictures of the composites. Figure 2 shows the TEM images of the unfilled and silica-filled epoxy nanocomposites. All of the images were magnified to 100,000×. These images show an agglomerate-free uniform dispersion of silica nanoparticles in epoxy up to a 10 wt % loading. For 20 wt % loading, we observed agglomerates of silica particles. So, we expected that at this loading, the mechanical properties would be low compared to those at the lower loading because agglomeration indicates filler–filler interaction and less filler–epoxy matrix interaction. The size of the majority of the nanoparticles was in the range 14–21 nm; this agreed with the supplier's data sheet.[20]

DSC

The influence of SiO_2 on the curing reaction and glass-transition behavior of the epoxy nanocomposites was investigated to understand molecular mobility in the nanocomposites. The DSC thermograms of the pure epoxy and epoxy–silica nanocomposites are shown in Figure 3. From the DSC plots (Fig. 3), the values of the onset temperature (T_o), peak temperature (T_p), and T_g were evaluated, and these values are tabulated in Table I. The measured T_g of the SC 79 epoxy resin, as shown in Table I, was 119°C. However, T_g of the epoxy–silica nanocomposites showed inconsistent behavior with various silica loadings. We observed an increase in T_g at a 10 wt % silica loading, and for other loadings, T_g was less than that of the pure epoxy. Obviously, the silica nanoparticles did not improve the thermal properties of the composite, except at a 10 wt % silica loading, where there was an increase of only 3°C. A slight influence in T_g was observed even at a high degree of filling. Recently, Sun et al.[4] also observed similar results and inferred that the T_g depression was related to the enhanced polymer dynamics due to the extra free volume at the resin–filler interface. Several other investigators observed significant reductions in T_g of SiO_2-modified epoxy composites.[5,12] These authors attributed the effects to the reduced crosslinking density in the composite; that is, the structure of the composite was altered by the presence of SiO_2 particles, for example, by the creation of additional free volume at the filler–matrix

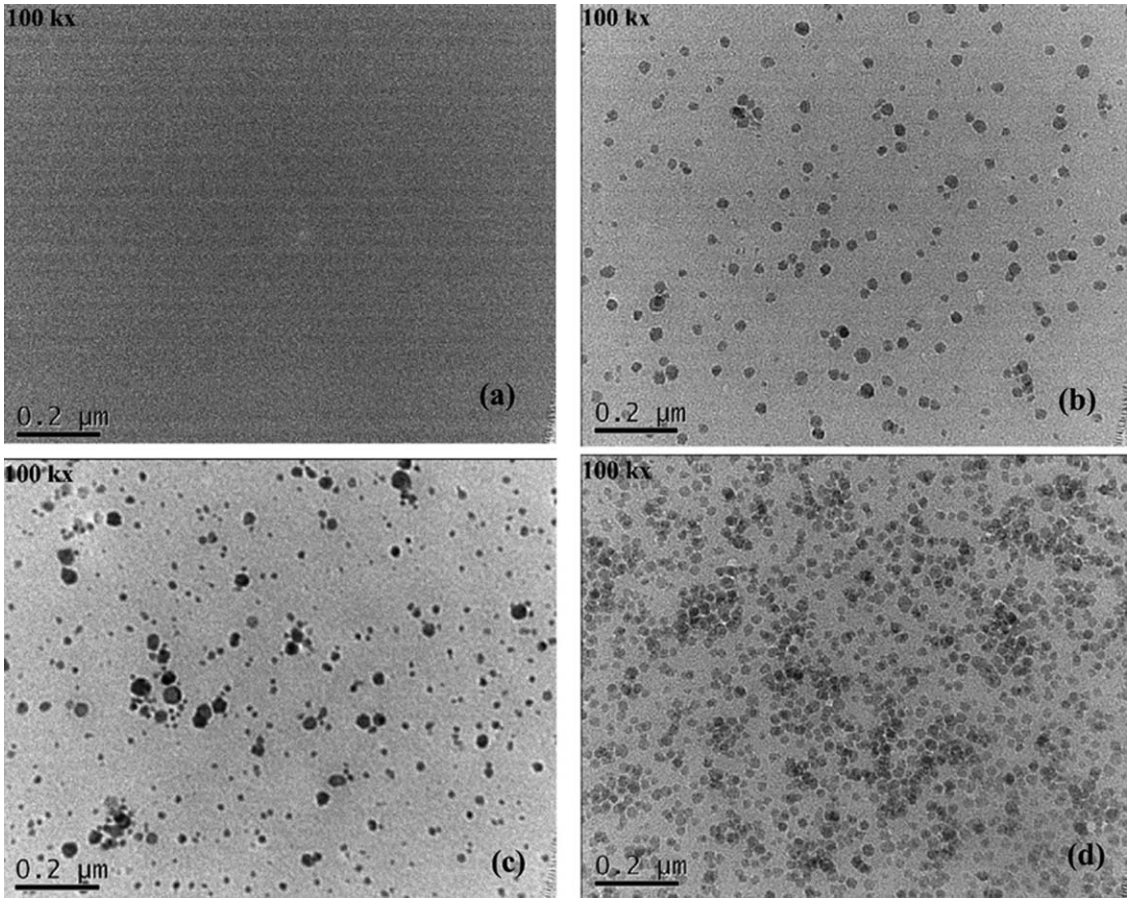

Figure 2 TEM images of the epoxy–silica nanocomposites: (a) pure epoxy and (b) 5, (c) 10, and (d) 20 wt % silica.

interface. In this study, we observed directly evidence for this from free-volume data (Table II), and none of the previously published data provided this unique information. Earlier, it was assumed that the particles were surrounded by a softer polymer shell and the strength of the composites increased with increasing distance from the surface of the particles.[23]

Mechanical properties

The ultimate tensile strength and tensile modulus were measured as per ASTM D 638-03 standards. The ultimate tensile strength of the SiO_2-filled epoxy composites as a function of filler loading are listed in Table II. The ultimate tensile strength value increased with filler loading up to 10 wt %, and thereafter, it decreased. Similar behavior was seen for hardness and strain at break values, but these values were higher than those of the pure epoxy. Therefore, we concluded that the SiO_2-filled epoxy composite with a 10 wt % filler content was stiffer and tougher than the composites with higher silica contents and, also, pure epoxy, and as such, 10 wt % filler was the optimum value of loading to produce composites with better mechanical properties.

Now, let us understand how these improved properties resulted from silica loading. It is known that the ultimate tensile strength of a particulate composite usually decreases with filler content, as reported by several authors, and it follows a power law in the case of poor filler/matrix bonding.[24,25]

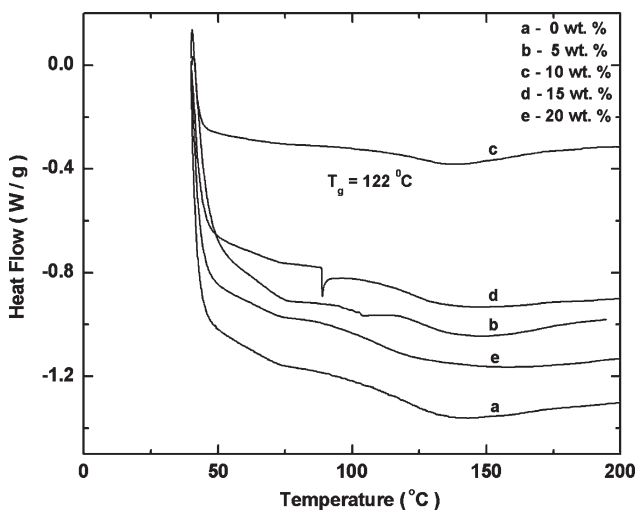

Figure 3 DSC thermograms of the pure epoxy and epoxy–silica nanocomposites.

TABLE I
DSC Results for the Epoxy–Silica Nanocomposites

SiO_2 content (wt %)	Transition temperatures (°C)					$\Delta H \pm 1.0$ (J/g)
	T_0	T_p	T_c	$T_c - T_0$	$T_g \pm 1.0$ (°C)	
0	116	130	153	36	119	378
5	118	134	150	32	118	350
10	122	143	157	35	122	331
15	120	133	151	31	118	301
20	117	131	150	33	115	265

T_0 = onset temperature, T_c = completion temperature, DH = change in enthalpy.

Theoretically, the ultimate tensile strength of the composite is expected to be lower than that of the unfilled polymer because the particles are unable to transfer the load during tensile loading.[26] Contrary to this, we obtained the opposite results, as shown in Table II. This indicates that the increase in the ultimate tensile strength with the addition of filler up to 10 wt % silica was due to the interaction between the filler and the matrix.[26] As a result, this interaction resulted in better stress transfer between the filler particles and the matrix and, thus, enhanced the ultimate tensile strength of the composite. This result was in agreement with the finding reported by Wu et al.[26] However, it was surprising that up to a filler loading of 10 wt %, the fractional free volume of the composites (described in the next section) increased; the opposite trend to that of the mechanical properties should have been observed. It is generally observed that both the hardness and the ultimate tensile strength exhibit opposite trends for free-volume change;[27,28] that is, as the strength increases due to specific interaction between the fillers and the matrix, the free volume of the composite shall decrease, but we observed that both the strength and free volume showed similar trends. The reason for an increase in the free volume is provided in a later section with the PALS results. The improvement in the mechanical properties (despite the free-volume increase) was attributed to the interaction established between the matrix and the surface-treated SiO_2. Recently, we showed that microparticles containing silica as a main component were able to establish some interaction with the epoxy matrix, where the strength of interaction was proportional to the silica content of the fillers.[29,30] On the other hand, a larger specific surface area of the nanofillers and the rigid nature of silica particles facilitated local bonds, which stabilized the structure and prevented material failure by limiting the propagation of cracks. Also, SiO_2 may not find its way to the free volume in the matrix because of its size and, hence, was located possibly between the chains of the epoxy matrix and, thereby, pushed the chains apart; this resulted in additional free volume.

Beyond a 10 wt % filler content, the ultimate tensile strength decreased. This was probably because of the decrease in the filler–matrix interaction by the effect of the agglomeration of filler particles, which caused premature failure. In general, the epoxy–SiO_2 composites showed improvement in the ultimate tensile strength over the range of filler contents studied compared to the pure epoxy resin.[31]

The results in Table II also show the tensile modulus monotonically increased with increasing filler loading. It is known that regardless of the particle size, a well dispersed system causes a reduction in the mobility and degree of short-range chain alignment, thus offering resistance to the movement of polymer chains under stress and, thus, increasing the modulus.[32] The slight increase in the matrix density was due to the higher density of the nanofiller particles used in this study.

TABLE II
Physical, Mechanical, and Free Volume Hole Size Properties of the Epoxy–Silica Nanocomposites

SiO_2 content (wt %)	Density ± 0.005 (g/cm^3)	Shore D hardness ± 2.0	Modulus (GPa)	Ultimate tensile strength (MPa)	Strain at break (%)	$V_f \pm 0.7$ (Å^3)
0	1.152	68.8	2.97	49.5	2.0	65.9
5	1.166	73.4	3.00	63.4	4.6	66.9
10	1.196	81.0	3.22	70.8	4.9	71.7
15	1.203	77.4	3.34	63.5	3.6	70.6
20	1.215	76.8	3.55	57.9	2.9	68.8

V_f = free volume hole size.

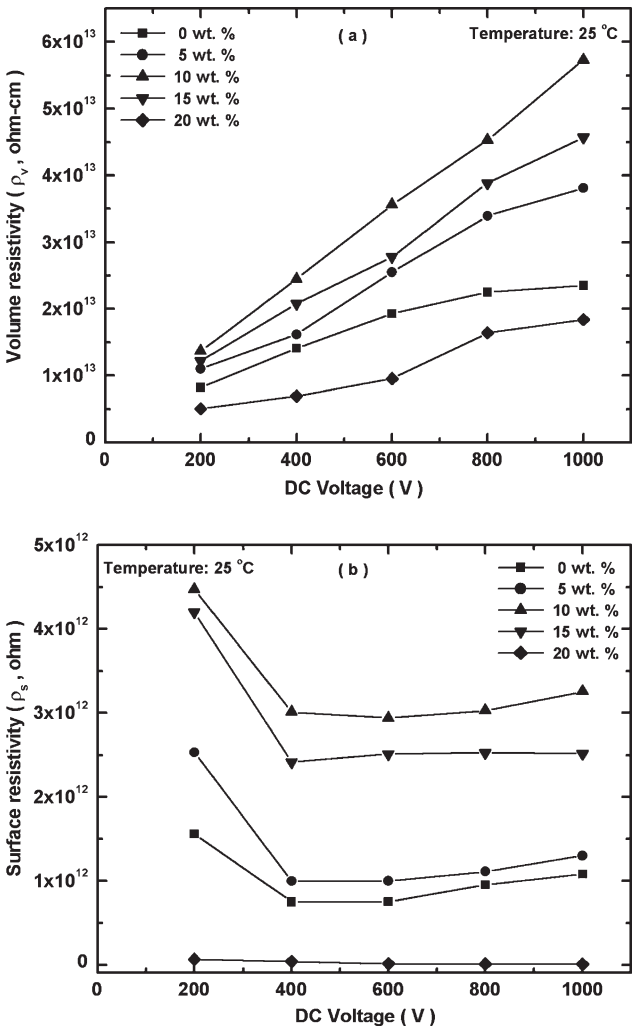

Figure 4 Effect of the dc potential on the epoxy–silica nanocomposites: (a) ρ_v and (b) ρ_s.

DC electrical resistivity (ρ_{dc}): Effect of the dc voltage and filler loading

The resistivity of an insulating material is due to the combined effects of the volume resistivity (ρ_v) and the surface resistivity (ρ_s), which always act in parallel. The ρ_v and ρ_s values of the pure epoxy and SiO_2-filled nanocomposites as a function of dc voltage are shown in Figure 4(a,b). As shown in Figure 4, ρ_v increased by 76% with increasing dc voltage for the 10 wt % epoxy–silica nanocomposites compared to the pure epoxy. In contrast, the ρ_s values for the 10 wt % epoxy–silica nanocomposites decreased by 53% with an increase in voltage from 200 to 400 V, and thereafter, it remained constant for the pure epoxy and epoxy–silica nanocomposites. It was also clear that the increase in ρ_v was large for the 10 wt % silica-filled nanocomposites. It was interesting to observe that at 20 wt % loading, the changes in ρ_v of the composite was less than that of the pure epoxy. The reason for this observation was probably due to the large number of nanoparticles in the epoxy matrix (particle agglomeration, as seen from the TEM images, and larger free volume of the composite compared to the pure epoxy) and greater mobility of charge carriers at this composition. Another possibility above a 10 wt % filler loading was the localized enhancement of electrical conductivity in the bulk of the epoxy composite. The effect of the filler loading on ρ_v seemed to be higher at 1000 V compared to 200 V, whereas no such effect was observed for ρ_s, probably because of the effect of the applied electric field. Because the field was greater, free charge carriers were generated from several sources in the material, such as the electrodes, fillers, and impurities present in the few monolayers of loose epoxy.[33] Because of the electrically conductive interface region, these free charge carriers were mobile in the bulk of the composite, and they tended to drift or migrate to the electrode of opposite polarity rather than accumulate at the

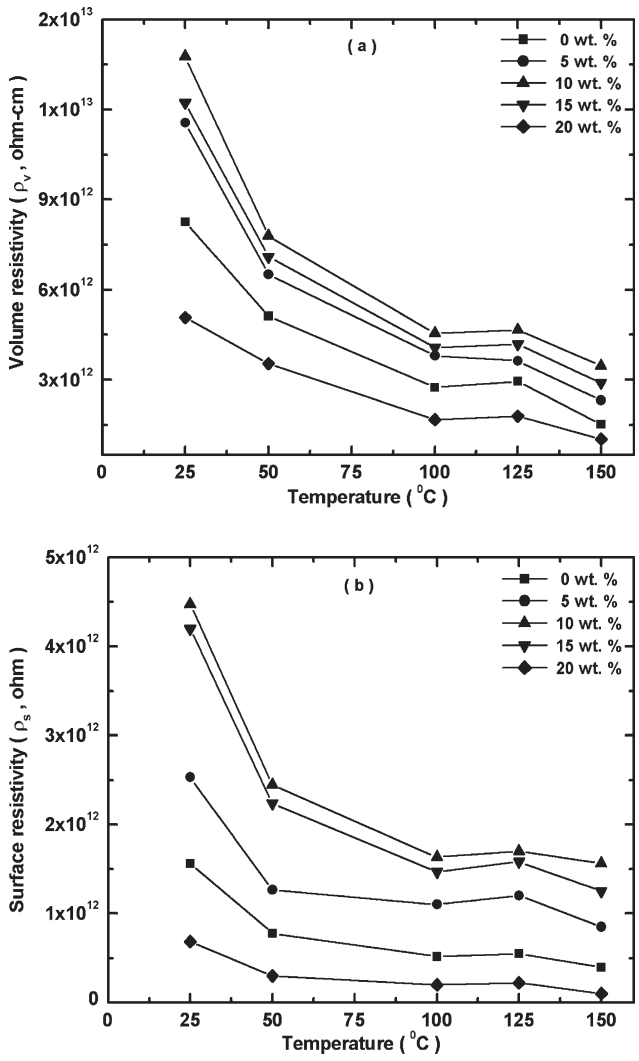

Figure 5 Effect of the temperature on the epoxy–silica nanocomposites: (a) ρ_v and (b) ρ_s.

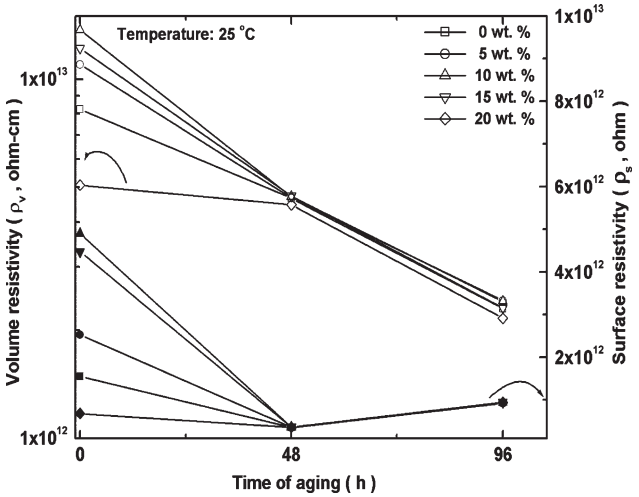

Figure 6 Effect of seawater aging on the epoxy–silica nanocomposites: (a) ρ_v and (b) ρ_s.

interface region; this explains the observed results.[33] Here again, the response of the 10 wt % filled nanocomposite was greater than those of the other samples.

Effect of temperature

The temperature dependences of ρ_v and ρ_s are shown in Figure 5(a,b), respectively. We observed that they decreased gradually over the temperature range studied. The reasons for the observed decrease in the resistivity with temperature were many. It was likely that ionic conduction became dominant because of activated molecular motion with increasing temperature up to 50°C and prominent up to 100°C. However, after this, they remained more or less constant. We know that the electrical conductivity of a polymeric material is a thermally activated process, which follows the well-known Arrhenius law.[34] As shown in Figure 5(a,b), at temperatures far below T_g (119°C), the interaction between macromolecules was quite intensive because of the thermosetting nature of epoxy resin, and we expected that the charge carriers were captured in deep-level traps. In this case, the behavior of dc resistivity for the cured epoxy system was considered to be dependent mainly on the change in the thermal activity of the carriers. The region from 100 to 125°C indicated that the polymer matrix underwent a phase change or the glass-transition process.[35] Above T_g, free and semifree charge carriers were created in the cured epoxy system so that the carrier density became higher and higher; together with the greatly increased mobility of the carriers as the temperature increased, this caused a quick decrease in the dc resistivity.[5]

Effect of seawater aging on ρ_v and ρ_s

When microelectronic devices are operated in a seawater environment, the environment certainly affects the insulating materials' characteristics. That was the reason for our study to understand the influence of seawater aging on ρ_v and ρ_s of the nanocomposites; the results are presented in Figure 6 for up to 96 h of aging. As shown in Figure 6, there was certainly a significant influence on the electrical resistivity. For epoxy and epoxy–silica nanocomposites, ρ_v decreased by 82 and 91% at 48 and 96 h, respectively, whereas ρ_s decreased by 87 and 67% at 48 and 96 h, respectively, of seawater aging. We observed that the decrease in ρ_s was very rapid in the 10 wt % filled composite up to 48 h of seawater aging, and then, the change was marginal. This was mainly due to the surface adhesion of the ions of seawater, and as such, the electrical conductivity increased or the resistivity decreased. Second, the free-volume results, as reported in the following section indicated that the 10 wt % filled nanocomposite had the largest free volume compared to the others, and hence, a quicker absorption and diffusion of seawater was possible. For seawater sorption, the rate of sorption was initially higher because of the ionic nature of water, and the conductivity increased or the resistivity decreased. As shown in Figure 6, ρ_v showed a continuous decrease up to 96 h, but ρ_s remained more or less constant after 46 h of aging. The constancy of ρ_s after 46 h of aging suggested saturation of the surface with ionic species, whereas ρ_v did not show such effects because it was the bulk parameter and the ions diffused further as the time of aging increased. The mechanism by which the decrease in the dc resistivity resulted may have been the following: The absorbed water was not in one layer but in different layers of the epoxy matrix, and therefore, the transfer of charge carriers occurred rapidly, and the conductivity increased. The first few water molecules may have been firmly bound to the nanoparticle. Other water molecules may have loosely been bound by van der Waals forces. Therefore, the concentration of water in the matrix may have been sufficient for conduction and likely provided a channel for charge carriers; this resulted in a decrease in ρ_v.[6] Secondly, the high polarity of the water molecules attracted charge carriers, particularly at the filler–matrix interface, and became significant; this resulted in a resistivity decrease.[36]

PALS

In brief, the positron lifetime method can be explained as follows: when an energetic positron enters a condensed medium, such as a polymer or a polymer composite, it thermalizes quickly and,

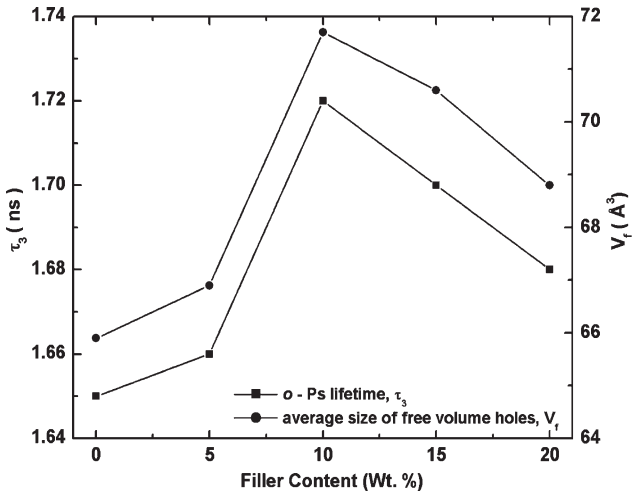

Figure 7 Plot of τ_3 and free-volume size as a function of the silica content for the epoxy nanocomposites.

thereafter, annihilates with an electron of the medium via free annihilation or from a localized state (trapped state) or forms a bound state with an electron called a *positronium* (Ps) atom. The free annihilation refers to positrons annihilating with an electron of the medium without getting trapped in defects of the medium. This lifetime is of the order 200 ps. Second, some of the positrons may get trapped in defects, such as voids in the crystalline regions, or at the interface and annihilate in a time ranging from 200 to 500 ps. The bound state of Ps can exist in two spin states. The para-positronium (in which the particle spins antiparallel) annihilates with a lifetime of 125 ps. The ortho-positronium (*o*-Ps) (in which the particle spins parallel) annihilates with a lifetime of 140 ns. In condensed matter, such as these samples, *o*-Ps annihilates mainly into two photons by a pickoff mechanism, in which the positron of *o*-Ps annihilates with an electron of opposite spin from the surrounding molecules. Thereby, its lifetime gets reduced to a few nanoseconds. The lifetime of *o*-Ps depends on the overlap of the Ps wave function with the electron wave function of the free-volume cavity. Hence, the larger the hole size is, the smaller the overlap is; hence, longer the lifetime is. So, the *o*-Ps pickoff lifetime (τ_3) and the intensity (I_3) of *o*-Ps are measures of the free-volume size and the number density, respectively.[21,22] As shown in Figure 7, the *o*-Ps lifetime and free-volume cell size increased with increasing filler content up to 10 wt %; thereafter, they showed a slight decreasing tendency. Free-volume cavities can exist both in the matrix and the matrix–filler interface regions. An increase in the free-volume cell size in the composite indicated that the addition of SiO_2 particles produced additional free volume apart from that already present in the matrix. This was because the average size of the filler was around 20 nm, and these did not localize in the existing free-volume cells and were located possibly between the chains of the epoxy matrix; they, thereby, pushed the chains apart and resulted in additional free volume. Because van der Waals forces operated between the chains, the SiO_2 particles found their way to such locations and, hence, increased the free volume. At higher filler loadings, that is, at 15 and 20 wt % silica, the decrease in the free volume could have possibly been due to the nonuniform distribution of the particles, which led to agglomeration and, hence, the result. This decrease in the free volume was from its value at 10 wt % silica, but it was certainly greater than that of the pure epoxy. By comparison, the uptake of seawater was greater in the 10 wt % silica-filled composite (as observed in the highest volume of the composite), mainly because of to the large free volume compared to the other samples. In Table II are listed the free-volume parameters along with ρ_v, hardness, and ultimate tensile strength as a function of the filler loading. As shown in Table II, all of the parameters increased up to a 10 wt % loading and, thereafter, showed a decreasing trend; this was discussed in the previous section.

CONCLUSIONS

On the basis of these results and this discussion, we concluded that the nanocomposites showed improved mechanical properties and high electrical resistivity for 10 wt % SiO_2. However, the thermal stability did not improve, but it did not deteriorate from the pure epoxy matrix, and as such, this makes the composite more suitable for a wide range of applications. It was evident that the effect of silica nanoparticles in the reactive epoxy resin incorporated via a sol–gel process improved the mechanical and electrical properties greatly. The dispersion of SiO_2 particles in the epoxy matrix, as revealed by TEM, were key for improving the properties. This was clear, as evidenced by agglomerate particles at 15 and 20 wt % loading; this showed a decrease in these properties. The ultimate tensile strength, hardness, and ρ_v increased by 43, 15, and 40%, respectively, for 10 wt % SiO_2 filler; this composite also had a larger free volume and higher conductivity or lower resistivity. ρ_v of the nanocomposites increased with dc voltage; on the other hand, the resistivity decreased with temperature and seawater aging. The free volume supported the decrease in the resistivity with seawater aging, and the expected correlation was found among the parameters, namely, the hardness, ultimate tensile strength, and free volume. This was possibly due to the bigger size of the nanoparticles. Finally, we concluded that 10 wt % SiO_2 seemed to be the optimum loading to produce

improved performance in the epoxy–SiO_2-filled nanocomposites.

The support and encouragement of the Center for Composite Materials Research (North Carolina Agricultural and Technical State University, Greensboro, NC), the Central Power Research Institute (Bengaluru, India), and the Mysore University Department of Physics (Mysore, India) in carrying out the experiments is greatly acknowledged. Thanks are also due to Suresha B. and Siddaramaiah for their valuable suggestions during the course of this study.

References

1. Ogata, N.; Jimmenez, G.; Kawaki, H.; Ogihara, T. J Polym Sci Part B: Polym Phys 1997, 35, 389.
2. Kingon, A. I.; Maria, J. P.; Streiffer, S. K. Nature 2000, 406, 1032.
3. Wilk, G. D.; Wallace, R. M.; Anthony, J. M. J Appl Phys 2001, 89, 5243.
4. Sun, Y. Y.; Zhang, Z.; Wong, C. P. Polymer 2005, 46, 2297.
5. Zheng, Y.; Chonung, K.; Wang, G.; Wei, P.; Jiang, P. J Appl Polym Sci 2008, 111, 917.
6. Zou, C.; Fothergill, J. C.; Rowe, S. W. IEEE Trans Dielectr Electr Insul 2008, 15, 106.
7. Kinloch, A. J.; Little, M. S. G.; Watts, J. F. Acta Mater 2000, 48, 4543.
8. Kinloch, A. J. Durability of Structural Adhesives, Applied Science Publishers: London, UK, 1983.
9. Ma, J.; Mo, M. S.; Du, X. S.; Rosso, P.; Friedrich, K.; Kuan, H. C. Polymer 2008, 49, 3510.
10. Rosso, P.; Ye, L.; Friedrich, K.; Sprenger, S. J Appl Polym Sci 2006, 100, 1849.
11. Blackman, B. R. K.; Kinloch, A. J.; Lee, J. S.; Taylor, A. C.; Agarwal, R.; Schueneman, G.; Sprenger, S. J Mater Sci 2007, 42, 7049.
12. Mahrholz, T.; Stängle, J.; Sinapius, M. Compos A 2009, 40, 235.
13. Liu, J.; Jean, Y. C.; Yang, H. Macromolecules 1995, 28, 5774.
14. Ramani, R.; Ranganathaiah, C. Polym Int 2001, 50, 237.
15. Ravikumar, H. B.; Kumaraswamy, G. N.; Thomas, S.; Ranganathaiah, C. Polymer 2005, 46, 2372.
16. Ravikumar, H. B.; Ranganathaiah, C.; Kumaraswamy, G. N., Siddaramaiah. J Mater Sci 2005, 40, 6523.
17. Applied Poleramic: Benicia, CA.
18. Technical Data Sheet for SC 79 Epoxy Resin; Applied Poleramic: Benicia, CA.
19. Nanoresins AG: Geesthacht, Germany.
20. Technical Data Sheet for Nanopox F400; Nanoresins AG: Geesthacht , Germany.
21. Chandrashekar, M. N.; Ranganathaiah, C. Colloids Surf B 2009, 69, 129.
22. Ranganathaiah, C.; Kumaraswamy, G. N. J Appl Polym Sci 2009, 111, 577.
23. Hartwig, A.; Sebald, M.; Kleemeier, M. Polymer 2005, 46, 2029.
24. Bikiaris, D. N.; Vassiliou, A.; Pavlidou, E.; Karayannidis, G. P. Eur Polym J 2005, 41, 1965.
25. Shuisheng, S.; Chunzhong, L.; Ling, Z.; Du, H. L.; Burnell-Gray, J. S. Eur Polym J 2006, 42, 1643.
26. Wu, C. L.; Zhang, M. Q.; Rong, M. Z.; Friedrich, K. Compos Sci Technol 2002, 62, 1327.
27. Hill, A. J.; Zipper, M. D.; Tant, M. R.; Stack, G. M.; Jordan, T. C.; Shultz, A. R. J Phys: Condens Matter 1996, 8, 3811.
28. Soares, B. G.; Almeida, M. S. M., Deepa Urs, M. V.; Kumaraswamy, G. N.; Ranganathaiah, C.; Siddaramaiah; Mauler, R. J Appl Polym Sci 2006, 102, 4672.
29. Altaweel, A. M. A. M.; Ranganathaiah, C.; Kothandaraman, B. J Adhes 2009, 85, 200.
30. Altaweel, A. M. A. M.; Ranganathaiah, C.; Kothandaraman, B.; Raj, J. M.; Chandrashekara, M. N. Polym Compos 2011, 32, 139.
31. Modesti, M.; Lorenzetti, A.; Bon, D.; Besco, S. Polymer 2005, 46, 10237.
32. Bhattacharya, S. N.; Kamal, M. R.; Gupta, R. K. Polymeric Nanocomposites: Theory and Practice; Hanser Gardener: Claremont, UK, 2008.
33. Singha, S.; Joy Thomas, M. IEEE Trans Dielectr Electr Insul 2009, 16, 531.
34. Mills, N. J. Plastics: Microstructure and Engineering Applications, 3rd ed.; Butterworth Heinemann: Oxford, 2005.
35. Dewsberry, R. J Phys D: Appl Phys 1976, 9, 2049.
36. Fabiani, D.; Montanari, G. C.; Testa, L.; Schifani, R.; Guastavino, F.; Bellucci, F.; Derosola, F. In Proceedings of the International Symposium on Electrical Insulating Materials, DIE, Univ. di Bologna, Bologna, Mie, Italy, Sept 2008; p 510